

# Nonlinear summation of force in cat soleus muscle results primarily from stretch of the common-elastic elements

THOMAS G. SANDERCOCK

Department of Physiology, Northwestern University Medical School, Chicago, Illinois 60611

Received 18 January 2000; accepted in final form 6 July 2000

**Sandercock, Thomas G.** Nonlinear summation of force in cat soleus muscle results primarily from stretch of the common-elastic elements. *J Appl Physiol* 89: 2206–2214, 2000.—The complex connective tissue structure of muscle and tendon suggests that forces from two parts of a muscle may not summate linearly. This study measured the nonlinear summation of force ( $F_{nl}$ ) in whole cat soleus during isometric and ramp movements. In six anesthetized cats, the soleus was attached to a servomechanism to control muscle length and record force. The ventral roots were divided into two bundles, each innervating about half the soleus; thus the two parts could be stimulated alone or together. In all experiments,  $F_{nl}$  was small (<6% of maximum tetanic tension). Peak  $F_{nl}$  occurred during changes in muscle force, either as a result of imposed muscle movement or the onset or offset of a stimulus train. The data were fit to a model in which both parts of the muscle were assumed to stretch to a common elasticity. The servomechanism was programmed to compensate for reduced stretch of the common elasticity during partial compared with whole muscle activation. These compensatory movements showed how the model could account for most, but not all, of  $F_{nl}$ .

tendon; architecture

CONTROL OF A MUSCLE DEPENDS in part on the recruitment and derecruitment of motor units. Because of the complex connective tissue matrix within a muscle (14, 20, 26, 33, 35), the effective mechanical properties of newly recruited motor units may depend on how much of the muscle is already active and to what degree these active fibers strain neighboring passive fibers and associated connective tissue and tendon. Little is known about the mechanical interaction of muscle fibers, and a quantitative measure of this interaction is essential for understanding how whole muscle properties arise from its constituent motor units.

Fibers within a muscle may mechanically interact in several ways. Even with the simplest possible model of muscle, that is, independent parallel fibers attached to an external tendon, activation of one fiber will stretch the tendon and affect the length and velocity of neighboring fibers (see Fig. 1A). Recent research has shown that the connective tissue structure of muscle is far more complex (Fig. 1B) (26, 33, 35). Proteins within the

muscle fibers are capable of transmitting lateral forces between myofibrils and to the extracellular connective tissue matrix pervasive throughout the muscle. The links between neighboring fibers may prevent sarcomere length heterogeneity observed in isolated fibers, thus preventing damage and altering muscle force (8, 21). In some muscles, fibers do not run the length of the muscle but rather rely on this extracellular matrix and other muscle fibers to transmit force (18, 24). Thus neighboring fibers are not mechanically independent. Additional sources of interaction between muscle fibers occur in the aponeurosis and tendon, where cross-links likely exist between tendon fibrils (33). Furthermore, in pennate muscle, when part of the muscle contracts, the angle of pennation of the remaining muscle fibers is likely to be altered (10, 36). It is not presently known which of these factors are functionally important.

One measure of the mechanical interaction between parts of a muscle, and the measure that will be used in this study, is the change of force produced by one part when another part of the muscle is active. This is commonly referred to as nonlinear summation. In this paper, nonlinear summation of force ( $F_{nl}$ ) will be defined as

$$F_{nl}(t) = F_{AB}(t) - F_A(t) - F_B(t) \quad (1)$$

$F_{AB}(t)$  is the force measured when both parts of the muscle are activated together.  $F_A(t)$  and  $F_B(t)$  are the force waveforms when *part A* and *part B*, respectively, are stimulated alone. Although the measure of  $F_{nl}$  is only an indirect measure of the strain throughout a muscle, it has the important advantage in that force is the key variable of interest in a systems' approach to motor control studies. Thus  $F_{nl}$  is a good functional representation of the total mechanical effects between parts of a muscle.

Nonlinear summation has been previously studied between parts of whole muscle during isometric (fixed end) contractions (4, 15) and between individual motor units during both isometric and slow ramp movements (7, 9, 27). In whole muscle studies, forces summed linearly during static isometric contractions. Linearity is surprising, considering the many ways fibers within a muscle can mechanically interact. This study ex-

Address for reprint requests and other correspondence: T. G. Sandercock, Dept. of Physiology, M211, Ward 5–295, Northwestern Univ. School of Medicine, 303 E. Chicago Ave., Chicago, IL 60611 (E-mail: t-sandercock@northwestern.edu).

The costs of publication of this article were defrayed in part by the payment of page charges. The article must therefore be hereby marked "advertisement" in accordance with 18 U.S.C. Section 1734 solely to indicate this fact.

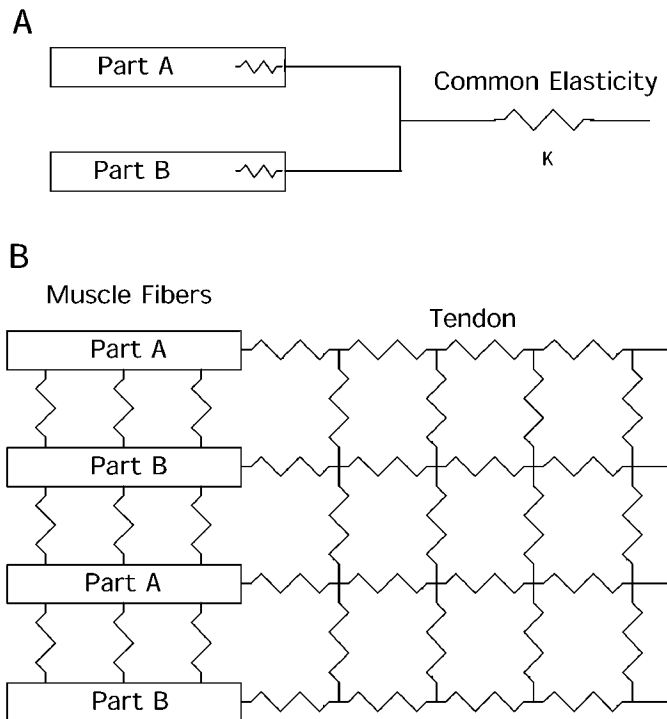


Fig. 1. Muscle and tendon models. A: simplified model of the common elasticity. *Part A* and *part B* refer to the muscle fibers in groups A and B, respectively. The elasticity of *part A* is attributed to the cross bridges within the muscle fibers, as well as elastic links within the fibers and between fibers and tendon, that act independently from *part B*. The common elasticity,  $K$ , refers to any elastic component that is stretched by the fibers in both *parts A* and *B*. B: detailed model with elastic links between fibers and tendons.

pands on those studies by examining nonlinear summation during dynamic movements. In contrast to whole muscle, motor unit summation has been shown to be quite nonlinear (7, 9, 27). However, single motor units represent a small portion of a muscle; thus sources of nonlinearity, such as compression of passive muscle, may be insignificant when larger parts of the muscle are active. For this reason, it seemed important to study  $F_{nl}$  using larger active portions of the muscle.

The purpose of this study was to measure the nonlinear interaction between two parts of cat soleus during static and dynamic conditions. The soleus was experimentally divided into two large pseudo-motor units by splitting the ventral roots into two bundles.  $F_{nl}$  was measured during equal-duration isometric tetani to each part of the muscle, different-duration tetani to each part of the muscle, and during stretches and releases of the muscle. Finally, the lumped parameter model of Fig. 1A was fit to the data to determine to what extent the model of Fig. 1A can account for the nonlinearity. Each part of the muscle was assumed to have its own independent-series elastic element (representing the elasticity of the cross bridges plus the independent portion of the tendon), which in turn connect to a common-series elasticity. The physical location of the common elasticity is not restricted to the external tendon but rather represents any compliance stretched by both parts of the muscle. The model was

shown to provide a good enough fit so more complex models may not be needed for most applications.

## METHODS

The data were obtained from six cats (male and female). All surgical and experimental procedures conformed with the policies of Northwestern University and the National Institutes of Health. The surgical procedures are only briefly summarized here because a detailed account was recently presented (30). The cats were anesthetized with isoflurane during the surgical procedures and switched to pentobarbital sodium for data collection. The left hind legs were partially denervated and mounted in a rigid frame. The nerve and blood supplies to the soleus were preserved. The calcaneus was cut and attached to a servomechanism (custom device with a compliance of 0.01 mm/N), allowing the soleus to be moved by computer while simultaneously measuring muscle force. Before the tendon was cut, the foot was manually dorsiflexed and a thread was tied to the tendons of both the soleus and medial gastrocnemius. After the soleus was attached to the puller, realignment of the threads was defined as maximum physiological length (0 mm).  $L_o$  is defined in this paper as the length at which peak isometric tetanic tension ( $P_o$ ) occurs. (This corresponds to  $L_o$  in Eq. 2.) The ventral roots were exposed via laminectomy and divided into two bundles, each part innervating roughly half of the soleus, and placed on separate hook electrodes so that each part could be stimulated independently. Stimulus isolation units were used, and the roots were stimulated using suprathreshold pulses 0.1 ms in duration and 2–10 V in amplitude. Stimulus trains were 100 Hz. The muscle force and length signals were generally sampled at 1 kHz, although for some quick stretches and releases sampling was at 10 kHz. Passive tension was always measured and subtracted from active tension.

Nonlinear summation was measured under three experimental conditions: 1) isometric contractions with equal-duration tetani to both parts of the muscle, 2) isometric contractions with unequal-duration tetani, simulating recruitment of new motor units to an already partially active muscle, and 3) quick stretches and releases of the muscle, simulating a changing external load. *Experiment 1* was selected because of its simplicity. *Experiments 2* and *3* were selected because they were expected to produce the largest nonlinear summation. All three experiments share a common protocol. First, the whole muscle was stimulated by activating the ventral roots for *part A* and *part B* simultaneously. Next, the ventral roots for *part A* and *part B* were stimulated individually, and muscle force was measured. The length of the muscle-tendon complex was the same in each of the three trials. Nonlinear summation error,  $F_{nl}$ , was defined by Eq. 1. It was essential that there was no cross-stimulation of the ventral roots. This possibility was ruled out because tetanic tension from the two parts of the muscle summed linearly to 0.5% when the muscle was stimulated near maximum physiological length, even when the stimulating voltage was increased by a factor of two. It is also critical that the muscle did not fatigue during the times when *parts A*, *B*, and *AB* were measured. This was not a problem in cat soleus because the muscle is resistant to fatigue and because 1-min rest intervals were allowed between trials. In every group of trials (*A*, *B*, and *AB*), at least one waveform was remeasured to test for fatigue. In some experiments, the measurements were made several times and the order of stimulation was varied. Waveforms were generally repeatable with errors <0.5% of maximum tetanic tension.

Some of the data were analyzed by constructing length-tension curves during whole or partial muscle stimulation. The data were fit to Otten's equation (3, 23)

$$f(x) = P_o \exp \left\{ - \left[ \frac{\left( \frac{x - L_o}{W + 1} \right)^{2.1527} - 1}{1.2857} \right]^{2.4649} \right\} \quad (2)$$

where  $f$  is force (in N),  $x$  is muscle length (in mm),  $L_o$  is the peak of the length-tension curve (in mm), and  $W$  is the width of the length tension curve (in mm). This empirical equation fit the soleus length tension data quite well by optimizing only three parameters:  $L_o$ ,  $W$ , and  $P_o$ . This procedure could detect small shifts in  $L_o$ .

To determine whether the common-elastic lumped parameter model of Fig. 1A provided a reasonable account of the data, the puller was used to mimic stretch of the common elasticity. The common elasticity was assumed to be a linear Hookian element ( $K$ ). When both halves of the muscle are active, the common elasticity will stretch by a distance ( $L_{AB}$ ) proportional to  $F_{AB}$

$$L_{AB}(t) = F_{AB}(t)/K \quad (3)$$

When *part A* is stimulated alone, the muscle fibers will not shorten as much, since now the common elasticity will only be stretched by the force from *part A*

$$L_A(t) = F_A(t)/K \quad (4)$$

Thus, for the muscle fibers of *part A* to shorten by the same amount when *part A* is stimulated alone, compared with when both parts of the muscle are active, the servomechanism needs to move by the difference between  $L_{AB}(t)$  and  $L_A(t)$ . This movement can be approximated by

$$L_B(t) = F_B(t)/K \quad (5)$$

The force waveform measured during activation of *part B* was divided by the estimated stiffness of the common elasticity. The resulting waveform is an approximation to the elastic stretch attributed to *part B*. It was used to drive the puller during activation of *part A*. Conversely, the force from *part A* was used to estimate the tendon stretch attributed to *part A* and used to drive the puller during activation of *part B* (Eq. 4). The summation of these two new waveforms was compared with the force from whole muscle stimulation to determine whether this could account for the nonlinearity. This procedure was repeated at both one-half and two times the initial estimate of  $K$ .

Quick stretches (0.5 mm in 5 ms) were used to measure muscle stiffness. Within this distance and time, the muscle acts as a linear spring, so the change in the force waveform is equal to the change in the length waveform multiplied by the stiffness ( $s$ ) (22). A computer program calculated the  $s$  that minimized the difference between the force and scaled length waveforms for the 5-ms period after the initiation of the stretch. This procedure provided a more accurate estimate of  $s$  than that obtained using a single-point measure 5 ms after stretch initiation.

The three-element model in Fig. 1A, coupled with the experimental stiffness measurements, can be used to determine the stiffness of the common elasticity. An algebraic solution was obtained by assuming that the common elasticity was to be linear over the range of forces measured ( $F_A$  to  $F_{AB}$ )

$$K = \frac{-s_A s_B - \sqrt{(s_A s_B)^2 + (s_{AB} - s_A - s_B)(s_{AB} s_A s_B)}}{s_{AB} - s_A - s_B} \quad (6)$$

where  $K$  is the stiffness of the common-elasticity and  $s_{AB}$ ,  $s_A$ , and  $s_B$  are the experimentally measured stiffness of the muscle when *parts AB*, *A*, and *B*, respectively, are stimulated with the same stimulus train.

## RESULTS

### Isometric contractions with equal-duration tetani.

Figure 2 shows nonlinear summation during an isometric contraction near  $L_o$ . Tetani of 100 Hz, from 200 to 600 ms, were delivered to *parts A*, *B*, and *AB* together. The resulting force waveforms are shown in Fig. 2, *top*. The mathematical subtraction of these waveforms ( $F_{nl}$ ) is shown in Fig. 2, *middle*. Overall  $F_{nl}(t)$  is quite small. The largest  $F_{nl}$  (0.65 N) is  $\sim 3\%$  of  $P_o$  (25 N) and occurs during tension development (200–350 ms) and tension relaxation (650–850 ms). Note that  $F_{nl}$  during the force plateau (500–600 ms) was near zero.

These results are consistent with the common elasticity model of Fig. 1A. During the rise of force, the common elasticity stretches more when both parts of the muscle are active, resulting in a higher velocity of

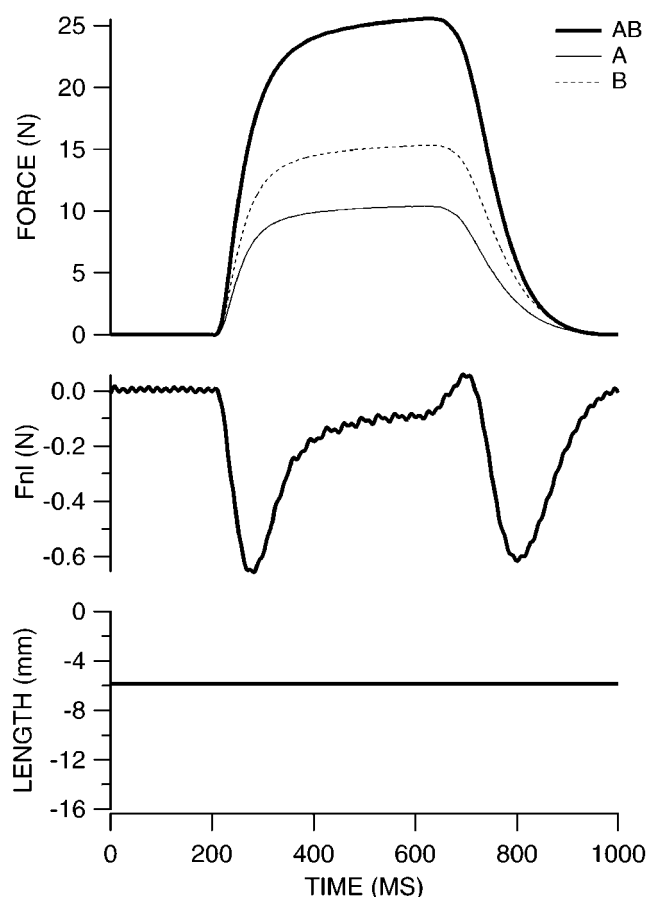


Fig. 2. *Top*: typical example of nonlinear summation during an isometric contraction. The heavy line *AB*, thinner line *A*, and dotted line *B* denote the forces from the whole muscle when ventral roots bundle *A* and *B* together, *A* alone, and *B* alone were stimulated, respectively (100 Hz, 0.2–0.6 s). *Middle* depicts nonlinear summation of force ( $F_{nl}$ ) as defined by Eq. 1 in the text. *Bottom* shows the length of the muscle-tendon complex. In this muscle, length where peak isometric tetanic tension occurs ( $L_o$ ) was  $-6.5$  mm.



shortening and hence a lower force. During the plateau, fiber velocity is near zero; therefore,  $F_{nl}$  will depend primarily on altered fiber lengths and the resulting shift along the length-tension curve. Because this contraction occurred near  $L_o$ ,  $F_{nl}$  is small. As shown below, steady-state  $F_{nl}$  increases at shorter or longer muscle lengths. During the fall in force,  $F_{nl}$  again becomes negative. This is probably due to a greater stretch velocity when both parts of the muscle relax together. Stretch during relaxation has been shown to cause muscle force to fall more rapidly (6).

To determine whether these results are quantitatively consistent with the common-elasticity model, the servomechanism was used to mimic stretch of the common elasticity. The common elasticity was estimated and used to compute movements for the servomechanism as described in Eqs. 4 and 5. Preliminary experiments showed that  $K$  was approximately equal to 20 N/mm. Values of  $K$  at 10 and 40 N/mm were also tried. Figure 3 shows the result using the same muscle as in Fig. 2. The solid light line shows  $F_{nl}$  when the estimated tendon stretch was based on a  $K$  of 20 N/mm. Note that the compensating movements of the servomechanism almost eliminated  $F_{nl}$  during the force-development and plateau phases. During the relaxation phase, substantial  $F_{nl}$  remained. The stiff  $K$  (40 N/mm) undercompensated. The compliant  $K$  (5 N/mm) overcompensated, except during the relaxation phase, where it minimized  $F_{nl}$ . Similar results were obtained on the one other cat subjected to this procedure.

The effect of muscle length on  $F_{nl}$  was studied using the same equal-duration tetani. At different muscle lengths, the shape of  $F_{nl}$  changed. Figure 4 shows typical  $F_{nl}$  waveforms during isometric contractions with the same 100-Hz trains described above. During force-development and plateau region phases,  $F_{nl}(t)$  became increasingly negative at shorter muscle lengths. This was observed in all muscles. The response was more variable during the relaxation phase. During relaxation, most muscles showed the greatest negative  $F_{nl}$  at long lengths. In general,  $F_{nl}$  was less

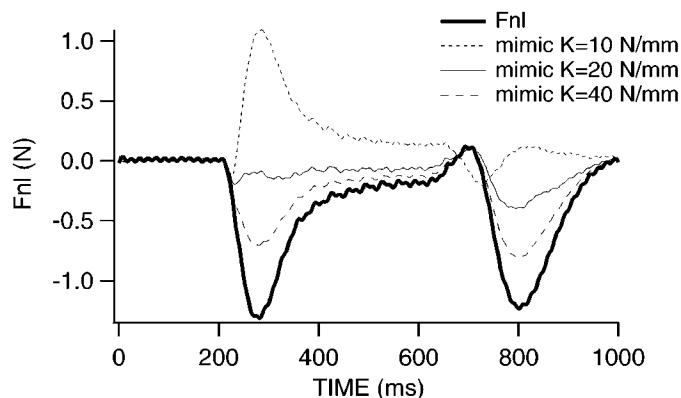


Fig. 3. Servo movement to compensate for stretch of common elasticity during equal duration tetani. Heavy line is  $F_{nl}$  redrawn from Fig. 2. Light lines show puller compensation for 3 different values of  $K$  (10, 20, and 40 N/mm).

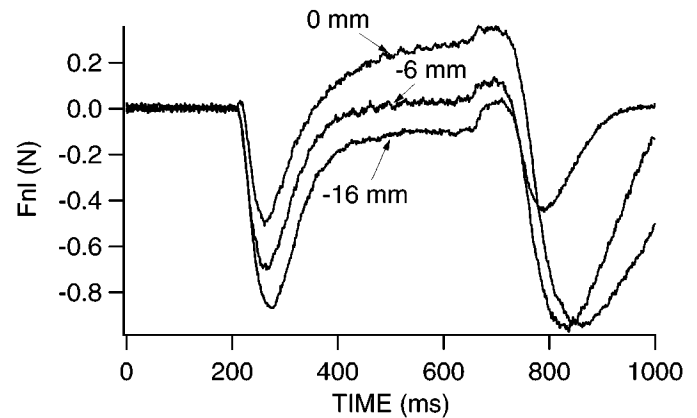


Fig. 4. Example of nonlinear summation during isometric contractions with equal duration tetani at different muscle lengths. Same duration tetani as in Fig. 2 were used.

negative and, in some muscles, even positive at short muscle lengths.

Partial activation of a muscle may not stretch the common elasticity as much as full activation. Therefore, when the muscle-tendon complex is held at a specific length, the muscle fibers will be longer during partial activation compared with during full activation; hence, a shift in the length-tension relationship to shorter lengths will occur during partial activation. To determine whether stretch of the common elasticity can be detected as a shift in the length-tension relationship, length-tension curves were constructed from data measured during whole and partial muscle stimulation. Force was measured every 2 mm, over a range from -16 to 0 mm, using 100-Hz trains 400 ms in duration. Force was measured on the plateau to minimize the dynamic effects of tendon stretch. The data were fit with Eq. 2. During partial muscle stimulation,  $L_o$  occurred at lengths  $0.76 \pm 0.38$  mm shorter than that for whole muscle. The shift in  $L_o$  was statistically significant ( $P < 0.001$ ,  $t$ -test, 1 tailed). When it is assumed that the tendon is linear in the region between  $F_A$  and  $F_{AB}$ , the shift can be used to estimate the stiffness of the common elasticity

$$K = (F_{AB} - F_A) / (L_{oAB} - L_{oA}) \quad (7)$$

The data for all six cats provided an estimate of common elasticity of  $11.7 \pm 4.94$  N/mm. Note that  $K$  estimated by using a shift in the length-tension curve is less than the  $K$  that provided the best fit when the puller was used to mimic tendon stretch. This is probably due to the nonlinear and history-dependent properties of the common elasticity (see DISCUSSION). In addition, the very small shifts in the length-tension curves make this estimate susceptible to noise.

*Isometric contractions with unequal-duration tetani.* The data above show that the maximum nonlinearities occurred during tension development and relaxation. Similar measurements were made during isometric contractions, except with unequal-duration tetani to each part of the muscle. The idea behind these experiments is that, if one part of a muscle contracts isomet-

rically, stimulation of the second part will further stretch the common elasticity, transiently shortening the already active fibers. The force-velocity properties of muscle suggest this should decrease force from the active part. In contrast, during relaxation, stretch of the active fibers will lead to a positive velocity and increased force. *Part A* was stimulated at 100 Hz from 0.05 to 1.0 s, and *part B* was stimulated at 100 Hz from 0.20 to 0.50 s. *Parts A* and *B* were again stimulated together and then by themselves. Figure 5 shows a typical result.  $F_{nl}(t)$  is quite small, with the peak  $<5\%$  of  $P_o$ . The peak  $F_{nl}$  occurred during the rise and fall of tension in *part B*. Note that, unlike the case with equal-duration tetani, here  $F_{nl}$  is positive during relaxation. The average peak  $F_{nl}(t)$  in six cats was  $3.6 \pm 1.8\%$  of  $P_o$ .

As before, the common-elasticity model was tested by using the servomechanism to mimic tendon stretch. Figure 6 depicts this procedure. The puller movements based on the estimated tendon stretch ( $K = 20$  N/mm) (bottom) and the force waveforms resulting from these movements (top) are both shown. The error was recalculated using these two waveforms and appears with the original  $F_{nl}$  (middle). Note that the error was sub-

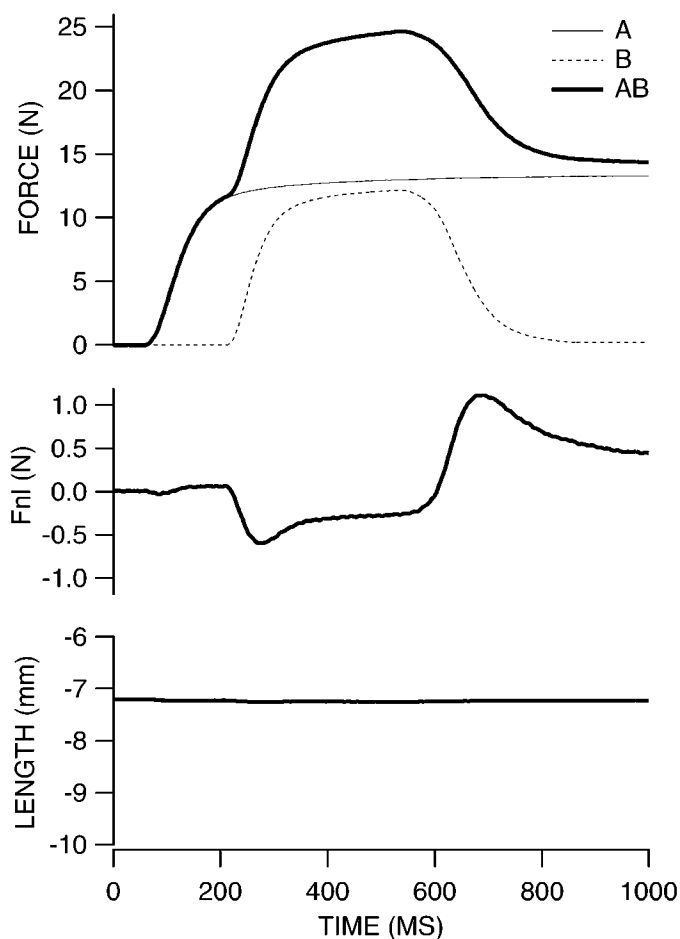


Fig. 5. Typical example of nonlinear summation during isometric contractions with different duration tetani. *Part A* was stimulated at 100 Hz from 0.05 to 1.0 s, and *part B* was stimulated at 100-Hz train from 0.2 to 0.5 s.

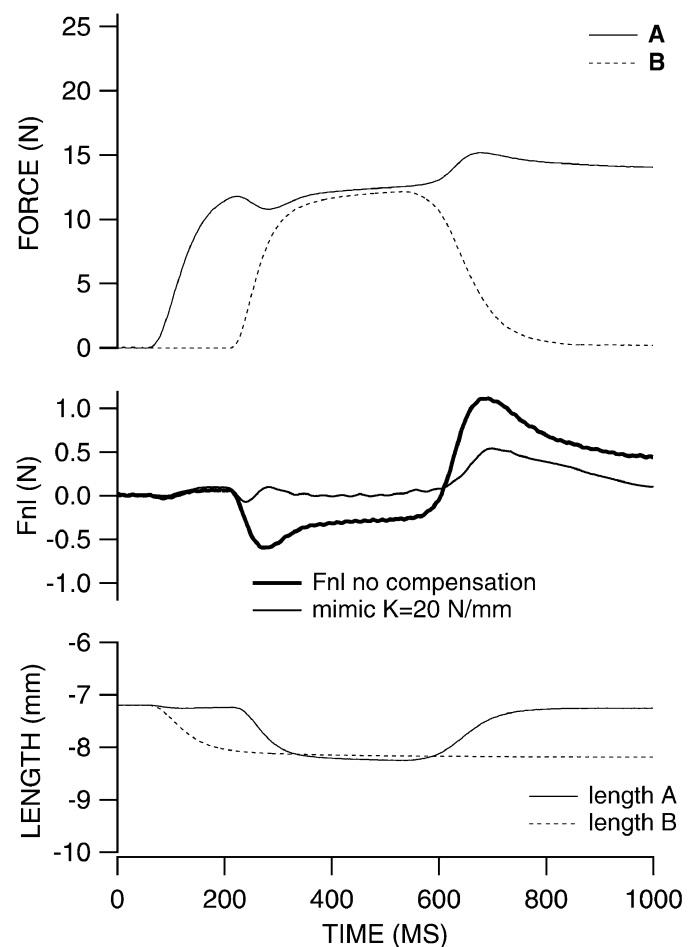


Fig. 6. Demonstration of servo movement to compensate for stretch of common elasticity during different duration tetani. Same muscle and stimulus patterns as in Fig. 5 were used. See text for details.

stantially reduced. Three different values for  $K$  were tried on the same muscle, and the results are shown in Fig. 7. Compensatory movements based on the stiffest tendon ( $K = 40$  N/mm) were not large enough to minimize the error. Compensation based on  $K = 20$  N/mm did a good job reducing the error during force develop-

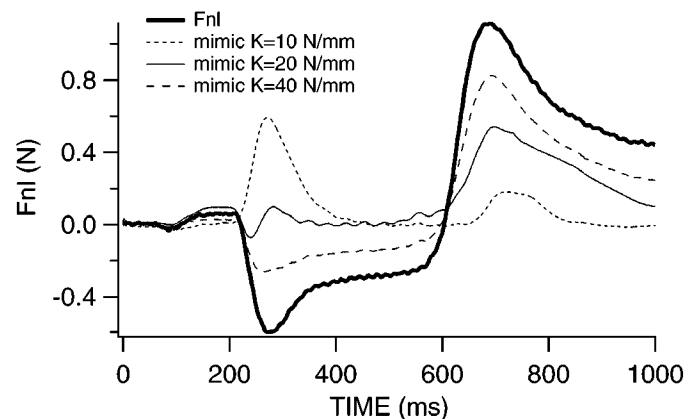


Fig. 7. Servo movement to compensate for stretch of common elasticity during different duration tetani. Same muscle as in Figs. 5 and 6 was used.

ment and the plateau region but only partially reduced the error during relaxation. Compensation using the most compliant value ( $K = 10$  N/mm) overcorrected during force development but provided a good match during force relaxation. Overall, for the example shown in Fig. 7, the mean square error was reduced 55% by  $K = 40$ , 81% by  $K = 20$ , and 90% by  $K = 10$  N/mm. Similar results were observed in muscles of all six cats. Generally, the error was most erratic during force relaxation.

Because a single value for  $K$  did not optimally correct for the complete waveform, three different regions were analyzed: 1) tension development (peak error between 200 and 300 ms), 2) plateau region (mean error between 500 and 550 ms), and 3) tension relaxation (peak error between 600 and 700 ms). The difference between the uncompensated  $F_{nl}$  and the compensated  $F_{nl}$  were measured at each of the three points and plotted as a function of  $K$ . The optimal value of  $K$  was selected by linear interpolation between points. The results based on six cats are as follows: 1) tension development  $K = 24.5 \pm 10.6$ , 2) plateau region  $K = 9.7 \pm 18.1$ , and 3) tension relaxation  $K = 10.4 \pm 4.8$ . These data are consistent with Fig. 7. Therefore, although the common-elasticity model qualitatively explains some of the error, the elasticity is not fully described by a linear elastic element.

**Nonlinear summation during muscle stretch or release.** Nonlinear summation was also measured during imposed increases or decreases in muscle length during stimulation at 100 Hz. Initial tests showed that moderate ramps ( $\pm 40$  mm/s or less) did not produce  $F_{nl}$  larger than isometric contractions with unequal-duration tetani. However, at speeds of 100 mm/s or greater, larger values of  $F_{nl}$  were produced. A typical example is shown in Fig. 8 in which the muscle was shortened by a ramp of 2 mm in 20 ms. Note the largest  $F_{nl}$  ( $-6\%$  of  $P_o$ ) occurred during the ramp. This is consistent with the common-elasticity model because more of the stretch will occur in the muscle fibers when only part of the muscle is active (the common elasticity is proportionally stiffer). Figure 9 shows a similar result when the muscle was stretched by 2 mm. The average peak nonlinearity in six cats, for a positive or negative 2-mm ramp, was  $6.5 \pm 1.2\%$  of  $P_o$ . Attempts to use the servomechanism to compensate for stretch of the common elasticity (as above in Fig. 6) were not successful due to limitations of the servomechanism.

Quick stretches were used to measure muscle stiffness when the whole muscle, *part A*, or *part B* was stimulated. Applying the model of Fig. 1A, these data enabled estimation of the common-elasticity stiffness using Eq. 6. On the basis of six cats, whole muscle stiffness was measured at  $10.38 \pm 3.16$  N/mm with common elasticity of  $22.25 \pm 5.08$  N/mm. By these calculations,  $0.46 \pm 0.07\%$  of the total muscle compliance can be attributed to the common elasticity during 100-Hz stimulation. The remainder is attributed to compliance of the cross bridges and the independent portion of the elasticity.

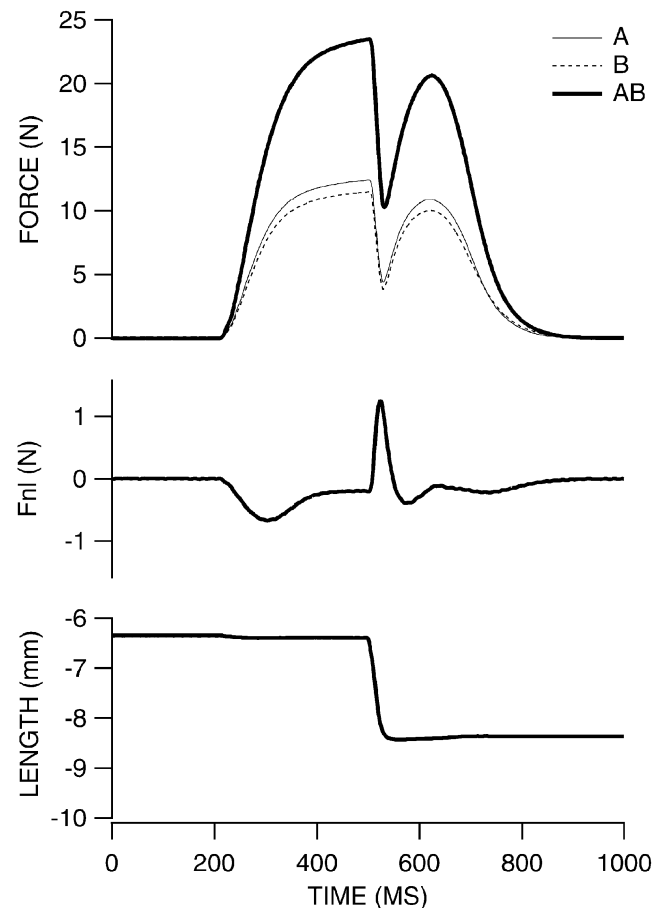


Fig. 8. Nonlinear summation during muscle movement. Similar to Fig. 2 except the stimulus is 100 Hz, 0.2–0.6 s, and the muscle is released with a ramp covering 2 mm in 20 ms.

## DISCUSSION

Cat soleus was divided into two functional parts by splitting the ventral roots into two bundles, each producing approximately the same force. Nonlinear summation between these parts was measured under three different experimental conditions. In all experiments, nonlinear summation was small,  $<7\%$  of  $P_o$ . The largest value of  $F_{nl}$  occurred during changes in muscle force, either due to activation or deactivation of part of the muscle or by imposed movements on the whole muscle.

There are surprisingly few studies that have examined the summation of force in muscle. This may result, on one hand, from viewing muscle fibers as parallel independent force generators, and, on the other hand, from knowing that the actual anatomy is so complex that a completely accurate anatomic model is out of reach. Early studies concerned with polyneuronal innervation of muscle fibers examined summation when the muscle was stimulated by the ventral roots (4, 15). These investigators found twitch summation less than linear. Brown and Mathews (4) correctly attributed this to stretch of the series elasticity. Rack and Westbury (29) used distributed stimulation to study the mechanical properties of cat soleus at low

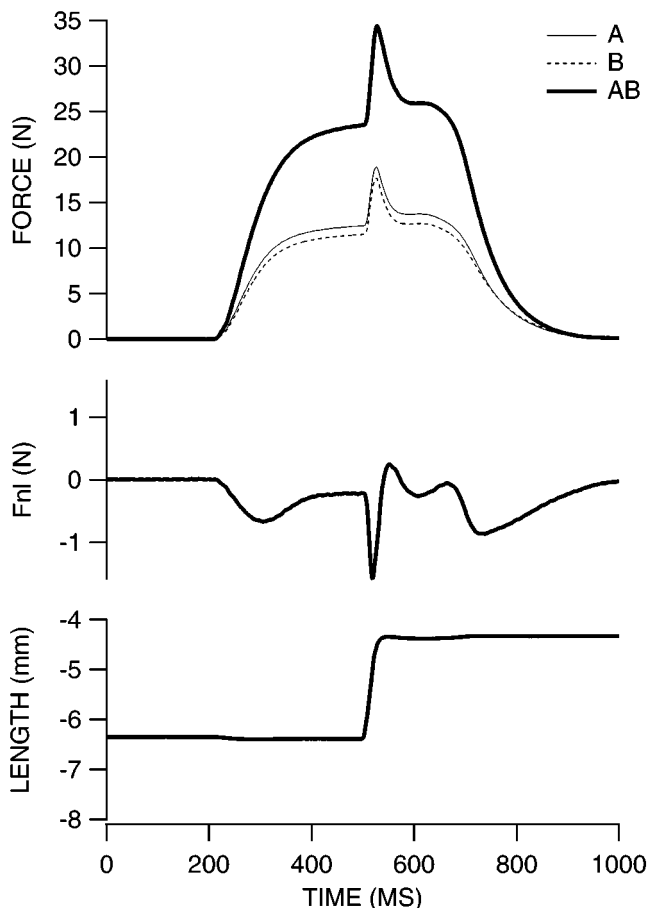


Fig. 9. Nonlinear summation during muscle movement. Experiment was similar to that in Fig. 8, except that the muscle was stretched 2 mm in 20 ms.

stimulation rates. They divided the ventral roots into five bundles and asynchronously stimulated each bundle so total muscle force was quite smooth compared with the unfused tetanus of each bundle. They noted that the average muscle force from the asynchronous stimulation was greater than the sum of each bundle stimulated separately. They speculated that the asynchronous stimulation reduced internal shortening of the fibers, preventing the breaking and reforming of the cross bridges, thus producing more tension. These studies are consistent with the data from this study.

Recent studies have demonstrated the nonlinear summation of force from individual motor units (7, 9, 11, 27). The underlying cause of the nonlinearity is not fully understood. It is likely caused by friction or elastic links between the relatively small number of active fibers in the motor units and the surrounding mass of passive fibers or other tissue. In this study, the ventral roots were divided into two bundles to form two large pseudo-motor units. Because the territory of a single motor unit can span almost the whole soleus (5), it can be assumed that the fibers for *part A* were randomly distributed between the fibers for *part B*. Thus nonlinear summation similar to that shown in motor units might have been observed in this study. However, the

nature of the nonlinearities observed was much different. In the motor unit studies, activation of a second motor unit often increased the force from the first, even after stimulation stopped in the second unit (7). Powers and Binder (27) showed that the nonlinearities diminished if the muscle was moved. Stretch and relaxation effects similar to those shown in Fig. 5 were not observed. Therefore, it seems that the cause of the nonlinearities in motor units relates more to the large mass of passive tissue and not to the stretch of the common elastic elements. Thus nonlinearities measured between single motor units probably do not have relevance to this study.

The angle of pennation of the muscle fibers may contribute to nonlinear summation, but it does not appear to be a major factor in this study. In a pennate muscle, such as the soleus, as more of the muscle contracts, the tendon stretches and the angle of pennation increases. The resulting force from the muscle is believed to decrease by the cosine of the angle of pennation. Therefore, pennation effects would be expected to produce a negative  $F_{nl}$  even during constant force contractions. In this study, the steady-state  $F_{nl}$  was small (plateau in Figs. 2, 4, 5, 8, and 9) and at least partially accounted for by the shift in the length-tension curve. Therefore, pennation effects do not account for substantial nonlinearity in cat soleus.

The mechanical links between fibers within a muscle may contribute to nonlinear summation of force. Recent research has shown that the force transmission in muscle is complex and incompletely understood (14, 26, 33, 35). It is generally agreed that cross-bridge connections between actin and myosin form the basis for active force generation (16). These cross bridges are an important part of the total muscle compliance. Titin also appears to be a significant load-bearing structure. It connects the myosin filaments to the Z disk and is probably responsible for most of the passive tension within a muscle (12, 13, 19). Other cytoskeletal proteins probably play roles in maintaining lattice structure (26). Intermediate filaments, desmin and skelamin, probably cross-link the myofibrils, keeping them in register (17). Regularly spaced costameres are probably the structures that transmit force between the myofibrils and the extracellular space (25). Thus, within the sarcolemma, the actin-myosin cross bridges and titin support longitudinal force transmission and other proteins are involved in transverse transmission of force. Outside the muscle fibers, there is a well-developed endomysial connective tissue matrix capable of transmitting muscle force (33, 34). Muscle fibers taper at their ending. Although there are specialized structures where they insert to the tendon plate, because the fibers always taper, the connective tissue matrix is likely to transmit some of the force. Furthermore, recent evidence shows that many muscles have fibers that do not run the length of the muscle (18, 20, 24). These fibers by necessity transmit their force to this endomysial connective tissue matrix. Street (32) recently demonstrated this transmission in frog fibers, which have a weaker endomysial matrix than mamma-



lian fibers. Thus force transmission in skeletal muscle is complex, far more complex than the common view of independent parallel fibers. It appears that muscle fibers are tightly linked to each other, which may affect the way force from parts of a muscle sum together. Despite the links between muscle fibers, the simple common-elasticity model of Fig. 1A fits the data reasonably well. A portion of the common elasticity measured in this study may be attributable to the links between muscle fibers.

Aponeurosis and tendon characteristics must also be considered when examining nonlinear summation. The external tendons of muscles have been studied *in vitro* by attaching them to pullers and studying their stress-strain characteristics. Generally, their properties have proven to be complex. The stress-strain relationship shows a toe region, where the tendon is quite compliant, followed by either an exponential or piecewise linear relationship until the stress becomes high enough that the tendon fails (36). The common-elasticity model used in this study assumed a linear  $K$  that may have contributed to the error. Studies have shown that tendons, when stretched to a length and held, exhibit creep over time, stretching with at least two different time constants (1, 36). In cycles of stretch and release, tendons show marked hysteresis, with release exhibiting less stiffness. This may explain why different values of  $K$  were needed to match the different regions of  $F_{nl}$  in Fig. 7. The tendon may be stiffer during stretch than during release. The problem with studying excised tendons is the difficulty attaching a cut tendon to a puller and knowing what part of the tendon is held firm and what part is allowed to stretch. In a careful study by Bennett et al. (2), attempts were made to determine whether the stress-strain relationship is constant for tendons of different mammalian species. They concluded that the difference between species was small compared with the error of measurement. They estimated compliance measurements were in error by a factor of two due to problems attaching the tendon to a measuring device. Scott and Loeb (31) measured the mechanical properties of aponeurosis and tendon in cat soleus using sonomicrometers and concluded that the mechanical properties were the same. This fits with the conclusion of Bennet et al., although there is probably at least as much problem attaching sonomicrometers to the tendon as Bennet et al. encountered in securing the cut end of a tendon. Thus uncertainty remains as to tendon and aponeurosis properties.

In this study, when the common-elasticity model was fit to the data, different values for  $K$  were derived, which were dependent on whether the movements were dynamic or static. The shift in the length-tension curve and compensation for tendon stretch during the plateau regions yielded an estimate of  $K$  of  $\sim 10$  N/mm. Estimates of  $K$  during tension development and quick stretches gave a  $K$  value  $> 20$  N/mm. These methods of estimating  $K$  are advantageous because they are non-invasive and because the parameter can be determined in a way muscle is normally used. The disadvantage is

that these methods are not direct measures of tendon strain; rather, they use the measured nonlinearity of summation to estimate common-elastic stretch. Small errors in measurement lead to large errors in stiffness estimates. This may explain why the common-elastic stiffness estimated via a shift in the length-tension curve was one-half that of the other two methods. Alternately, as mentioned above, tendon stiffness may be greater for dynamic stretch and thus a lower value during static length-tension measurements.

Estimates of common-elastic stiffness in this study agree closely with tendon stiffness measurements made using other techniques. Morgan (22) developed the alpha method to measure all the elasticity in a muscle other than that attributed to the cross bridges. In cat soleus, the total tendon stiffness was estimated to be 16.9 N/mm (22). This method is likely to measure some elastic elements that are not shared between the fibers and, therefore, not measured in this study. Rack and Westbury (28) used muscle spindles to estimate what they called the "entire tendon" in cat soleus. At 11 N, they estimated the tendon compliance to be 25 N/mm. This is close to the value of 24.5 N/mm obtained by mimicking tendon stretch during tension development and 22.5 N/mm estimated using quick stretches and algebraic calculations.

In this study, the common elasticity was measured during tetanic stimulation. Thus it was measured at relatively high force levels, ranging from about 50% of maximal tetanic force when half the muscle was stimulated to 100% of maximal tetanic force when both halves were active. As mentioned above, tendon properties are known to be nonlinear with greater compliance at low force levels (36). The elastic elements comprising the common elasticity may have similar properties. Thus, during natural activation at low firing rates, the common elasticity will probably be more compliant. However, the force during partial activation will also be less; thus fiber shortening, and therefore nonlinear summation, will not necessarily be greater than that measured in this study. Further work examining partial activation at subtetanic rates is necessary.

In conclusion, 1) the interaction (nonlinear summation of force) between two parts of cat soleus muscle was small. During isometric contractions the  $F_{nl}$  was  $< 3\%$  of  $P_o$ . 2) The largest nonlinearities occurred during dynamic changes in muscle force, resulting from the onset or offset of a stimulus train or movement of the muscle. Still, the  $F_{nl}$  was  $< 7\%$  of  $P_o$ . 3) Most of the nonlinear interaction can be explained by a simple lumped parameter model in which the interaction occurs through the stretch of a shared elastic elements (common elasticity). The stiffness of the common elasticity at maximum tetanic force was estimated at two times the stiffness of the whole muscle.

This work was supported by National Institute of Arthritis and Musculoskeletal and Skin Diseases Grant AR-34382



## REFERENCES

1. **Alexander RM.** Mechanics of skeleton and tendon. In: *Handbook of Physiology. The Nervous System. Motor Control*. Bethesda, MD: Am. Physiol. Soc., 1981, sect. 1, pt. 1, chapt. 2, p. 17–42.
2. **Bennett MB, Ker RF, Dimery NJ, and Alexander RM.** Mechanical properties of various mammalian tendons. *J Zool Lond* 209: 537–548, 1986.
3. **Brown IE, Scott SH, and Loeb GE.** Mechanics of feline soleus. II. Design and validation of a mathematical model. *J Muscle Res Cell Motil* 17: 221–233, 1996.
4. **Brown MC and Mathews PBC.** An investigation into the possible existence of polyneuronal innervation of individual skeletal muscle fibers in certain hind-limb muscles of the cat. *J Physiol (Lond)* 151: 436–457, 1960.
5. **Burke RE.** Motor units: anatomy, physiology, and functional organization. In: *Handbook of Physiology. The Nervous System. Motor Control*. Bethesda, MD: Am. Physiol. Soc., 1981, sect. 1, pt. 1, chapt. 10, p. 345–422.
6. **Caputo C, Edman KA, Lou F, and Sun YB.** Variation in myoplasmic  $\text{Ca}^{2+}$  concentration during contraction and relaxation studied by the indicator fluo-3 in frog muscle fibres. *J Physiol (Lond)* 478: 137–148, 1994.
7. **Clamann HP and Schelhorn TB.** Nonlinear force addition of newly recruited motor units in the cat hindlimb. *Muscle Nerve* 11: 1079–1089, 1988.
8. **Edman KA and Reggiani C.** Redistribution of sarcomere length during isometric contraction of frog muscle fibres and its relation to tension creep. *J Physiol (Lond)* 351: 169–198, 1984.
9. **Emonet-Denand F, Laporte Y, and Proske U.** Summation of tension in motor units of the soleus muscle of the cat. *Neurosci Lett* 116: 112–117, 1990.
10. **Gans C and Gaunt AS.** Muscle architecture in relation to function. *J Biomech* 24: 53–65, 1991.
11. **Heckman CJ, Weytjens JL, and Loeb GE.** Effect of velocity and mechanical history on the forces of motor units in the cat medial gastrocnemius muscle. *J Neurophysiol* 68: 1503–1515, 1992.
12. **Horowitz R, Kempner ES, Bisher ME, and Podolsky RJ.** A physiological role for titin and nebulin in skeletal muscle. *Nature* 323: 160–164, 1986.
13. **Horowitz R and Podolsky RJ.** The positional stability of thick filaments in activated skeletal muscle depends on sarcomere length: evidence for the role of titin filaments. *J Cell Biol* 105: 2217–2223, 1987.
14. **Huijing PA.** Muscle as a collagen fiber reinforced composite: a review of force transmission in muscle and whole limb. *J Biomech* 32: 329–345, 1999.
15. **Hunt CC and Kuffler SW.** Motor innervation of skeletal muscle: multiple innervation of individual muscle fibres and motor unit function. *J Physiol (Lond)* 126: 293–303, 1954.
16. **Huxley AF.** Muscle structure and theories of contraction. *Prog Biophys Biophys Chem* 7: 257–318, 1957.
17. **Lazarides E.** Intermediate filaments as mechanical integrators of cellular space. *Nature* 283: 249–256, 1980.
18. **Loeb GE, Pratt CA, Chanaud CM, and Richmond FJ.** Distribution and innervation of short, interdigitated muscle fibers in parallel-fibered muscles of the cat hindlimb. *J Morphol* 191: 1–15, 1987.
19. **Magid A and Law DJ.** Myofibrils bear most of the resting tension in from skeletal muscle. *Science* 230: 1280–1282, 1985.
20. **Monti RJ, Roy RR, Hodgson JA, and Edgerton VR.** Transmission of forces within mammalian skeletal muscles. *J Biomech* 32: 371–380, 1999.
21. **Morgan DL.** New insights into the behavior of muscle during active lengthening. *Biophys J* 57: 209–221, 1990.
22. **Morgan DL.** Separation of active and passive components of short-range stiffness of muscle. *Am J Physiol Cell Physiol* 232: C45–C49, 1977.
23. **Otten E.** Concepts and models of functional architecture in skeletal muscle. *Exerc Sport Sci Rev* 16: 89–137, 1988.
24. **Ounjian M, Roy RR, Eldred E, Garfinkel A, Payne JR, Armstrong A, Toga AW, and Edgerton VR.** Physiological and developmental implications of motor unit anatomy. *J Neurobiol* 22: 547–559, 1991.
25. **Pardo JV, Siliciano JD, and Craig SW.** A vinculin-containing cortical lattice in skeletal muscle: transverse lattice elements (“costameres”) mark sites of attachments between myofibrils and sarcolemma. *Proc Natl Acad Sci USA* 80: 1008–1012, 1983.
26. **Patel TJ and Lieber RL.** Force transmission in skeletal muscle: from actomyosin to external tendons. *Exerc Sport Sci Rev* 25: 321–363, 1997.
27. **Powers RK and Binder MD.** Summation of motor unit tensions in the tibialis posterior muscle of the cat under isometric and nonisometric conditions. *J Neurophysiol* 66: 1838–1846, 1991.
28. **Rack PM and Westbury DR.** Elastic properties of the cat soleus tendon and their functional importance. *J Physiol (Lond)* 347: 479–495, 1984.
29. **Rack PMH and Westbury DR.** The effects of length and stimulus rate on tension in the isometric cat soleus muscle. *J Physiol (Lond)* 204: 443–460, 1969.
30. **Sandercock TG and Heckman CJ.** Force from cat soleus muscle during locomotor-like movements: experimental data versus Hill-type model predictions. *J Neurophysiol* 77: 1538–1552, 1997.
31. **Scott SH and Loeb GE.** The mechanical properties of the aponeurosis and tendon of the cat soleus muscle during whole-muscle isometric contractions. *J Morphol* 224: 73–86, 1995.
32. **Street SF.** Lateral transmission of tension in frog myofibers: a myofibrillar network and transverse cytoskeletal connections are possible transmitters. *J Cell Physiol* 114: 346–364, 1983.
33. **Trotter JA.** Functional morphology of force transmission in skeletal muscle. *Acta Anat (Basel)* 146: 205–222, 1993.
34. **Trotter JA and Purslow PP.** Functional morphology of the endomysium in series fibered muscles. *J Morphol* 212: 109–122, 1992.
35. **Trotter JA, Richmond FJR, and Purslow PP.** Functional morphology and motor control of series-fibered muscle. *Exerc Sport Sci Rev* 23: 167–213, 1995.
36. **Zajac FE.** Muscle and tendon: properties, models, scaling, and application to biomechanics and motor control. *Crit Rev Biomed Eng* 17: 359–411, 1989.